remote sensing

MDPI

Article

Creating a Detailed Wetland Inventory with Sentinel-2 Time-Series Data and Google Earth Engine in the Prairie Pothole Region of Canada

Evan R. DeLancey [1,2,*], Agatha Czekajlo [1], Lyle Boychuk [3], Fiona Gregory [1], Meisam Amani [4], Brian Brisco [5], Jahan Kariyeva [1] and Jennifer N. Hird [1]

[1] Alberta Biodiversity Monitoring Institute, University of Alberta, Edmonton, AB T6G 2E9, Canada; a.czekajlo@alumni.ubc.ca (A.C.); fiona.gregory@ualberta.ca (F.G.); kariyeva@ualberta.ca (J.K.); jennifer.hird@ualberta.ca (J.N.H.)
[2] NGIS EU Limited, Ulysses House, D01 W2T2 Dublin, Ireland
[3] Prairie Region, Ducks Unlimited Canada, Regina, SK S4R 8P8, Canada; l_boychuk@ducks.ca
[4] Wood Environment and Infrastructure Solutions, Ottawa, ON K2E 7L5, Canada; meisam.amani@woodplc.com
[5] Canada Center for Mapping and Earth Observation, Ottawa, ON K1S 5K2, Canada; brian.brisco@canada.ca
* Correspondence: evan.delancey@ngis.ie

Abstract: Wetlands in the Prairie Pothole Region (PPR) of Canada and the United States represent a unique mapping challenge. They are dynamic both seasonally and year-to-year, are very small, and frequently altered by human activity. Many efforts have been made to estimate the loss of these important habitats but a high-quality inventory of pothole wetlands is needed for data-driven conservation and management of these resources. Typical landcover classifications using one or two image dates from optical or Synthetic Aperture Radar (SAR) Earth Observation (EO) systems often produce reasonable wetland inventories for less dynamic, forested landscapes, but will miss many of the temporary and seasonal wetlands in the PPR. Past studies have attempted to capture PPR wetland dynamics by using dense image stacks of optical or SAR data. We build upon previous work, using 2017–2020 Sentinel-2 imagery processed through the Google Earth Engine (GEE) cloud computing platform to capture seasonal flooding dynamics of wetlands in a prairie pothole wetland landscape in Alberta, Canada. Using 36 different image dates, wetland flood frequency (hydroperiod) was calculated by classifying water/flooding in each image date. This product along with the Global Ecosystem Dynamics Investigation (GEDI) Canopy Height Model (CHM) was then used to generate a seven-class wetland inventory with wetlands classified as areas with seasonal but not permanent water/flooding. Overall accuracies of the resulting inventory were between 95% and 96% based on comparisons with local photo-interpreted inventories at the Canadian Wetland Classification System class level, while wetlands themselves were classified with approximately 70% accuracy. The high overall accuracy is due, in part, to a dominance of uplands in the PPR. This relatively simple method of classifying water through time generates reliable wetland maps but is only applicable to ecosystems with open/non-complex wetland types and may be highly sensitive to the timing of cloud-free optical imagery that captures peak wetland flooding (usually post snow melt). Based on this work, we suggest that expensive field or photo-interpretation training data may not be needed to map wetlands in the PPR as self-labeling of flooded and non-flooded areas in a few Sentinel-2 images is sufficient to classify water through time. Our approach demonstrates a framework for the operational mapping of small, dynamic PPR wetlands that relies on open-access EO data and does not require costly, independent training data. It is an important step towards the effective conservation and management of PPR wetlands, providing an efficient method for baseline and ongoing mapping in these dynamic environments.

Keywords: wetlands; Sentinel-2; Google Earth Engine; Prairie Pothole Region; Canada; time-series; water dynamics

Citation: DeLancey, E.R.; Czekajlo, A.; Boychuk, L.; Gregory, F.; Amani, M.; Brisco, B.; Kariyeva, J.; Hird, J.N. Creating a Detailed Wetland Inventory with Sentinel-2 Time-Series Data and Google Earth Engine in the Prairie Pothole Region of Canada. *Remote Sens.* **2022**, *14*, 3401. https://doi.org/10.3390/rs14143401

Academic Editor: Dino Ienco

Received: 26 May 2022
Accepted: 12 July 2022
Published: 15 July 2022

1. Introduction

The Prairie Pothole Region (PPR) in the northern Great Plains of North America is a unique wetland region characterized by small depressional wetlands, called potholes, which have distinct seasonal cycles; they experience flooding in the spring due to snow melt and drying in the fall. These wetlands are particularly important for migratory waterfowl [1], temporary storm ponds for flood remediation, and water resources during droughts [2]. These wetland habitats are typically hydrologically closed [3,4], which makes them sensitive to short- and long-term climate changes. Despite their ecological importance and their valuable services, it has been estimated that 40–90% of pothole wetlands have been destroyed/drained [5,6]. This habitat loss value significantly varies because there has not been a decent baseline inventory of these wetland habitats across the whole PPR. This highlights the need for an up-to-date inventory of pothole wetlands to allow for data-driven conservation of these areas.

In Canada, a substantial amount of research has been conducted to allow for operational mapping and monitoring of wetlands. Typically, wetland inventories are produced at the wetland class or form level according to the Canadian/Alberta Wetland Classification System (CWCS/AWCS) [7] (Table 1). Wetland type is generally not considered for large-scale classifications as water permanence is difficult to capture with modern mapping techniques. Additionally, shallow open water is usually left out of these inventories as water depth is difficult to detect through photo-interpretation or satellite data. The PPR region of Canada is unique as the vast majority (>99%) of the wetlands are the swamp or marsh class, whereas peatlands (i.e., fens and bogs) are often only found in the Boreal transition areas. Overall, the generation of wetland inventories in the PPR should focus on the classification of marshes/swamps and separating these from permanent open water.

Table 1. Wetland classes, forms, and water permanence types relevant to the Prairie Pothole Region, according to the Alberta Wetland Classification System. The Canadian Wetland Classification System (CWCS) is based on the classes shown in the first column below. Adapted from: [8].

Class	Forms	Water Permanence Types [1]
Marsh	Graminoid	Temporary [II]
		Seasonal [III]
		Semi-permanent [IV]
Swamp	Wooded, coniferous	
	Wooded, mixedwood	
	Wooded, deciduous	
	Shrubby	Temporary [II] [2]
		Seasonal [III] [2]
Shallow Open Water	Subersed and/or floating aquatic vegetation	Seasonal [III]
		Semi-permanent [IV]
		Permanent [V]
		Intermittent [VI]
	Bare	Seasonal [III]
		Semi-permanent [IV]
		Permanent [V]

[1] Roman numerals for wetland permanence types relate to wetland classes as outlined in [9].

[2] Swamp water permanence types are only applicable to shrubby swamps given a current a lack of available information on wooded swamp types.

For proper conservation of PPR wetlands, a baseline inventory of their spatial boundaries and extents are needed. However, accomplishing this task over large areas can be challenging. From a mapping perspective, these wetlands are very dynamic both seasonally and annually, typically very small (below 0.1 ha), and often altered by human land-use activities. Addressing these mapping challenges using remote sensing is frequently done, given the advantages of these approaches (e.g., higher cost effectiveness and broader coverage than field methods). A recent, updated review of remote sensing approaches to PPR mapping is provided by Montgomery et al. [10], wherein the authors offer a comprehensive perspective on the topic.

Good inventory data of PPR wetlands can be obtained through high-resolution photo-interpretation, such as the data provided in Duck Unlimited Canada's (DUC) high-resolution mapping program [11]. However, generating these data over large areas (e.g., whole provinces or states) is typically expensive and time-consuming. Other wetland large-scale classification methods using Earth observation (EO) data, such as those acquired by Landsat, Sentinel-1/2, or SPOT [12–16], have produced promising results in less dynamic wetland landscapes (i.e., boreal or forested ecosystems). However, these methods tend to miss many of the temporary/seasonal wetlands in the PPR due to the static nature of most landcover classifications. Additionally, open-access EO data (e.g., Landsat, Sentinel-2) typically do not provide high enough resolution to capture these very small wetland features [17].

The training of a wetland classification model in the PPR is also troublesome. Datasets that are normally considered to be high-quality training for landcover classifications, such as the Alberta Biodiversity Monitoring Institute's (ABMI) photoplots [18] used in wetland/landcover studies such as in Castilla et al. [12], Hird et al. [15], and others [19–23], do not appear to be very useful in the PPR. These data contain over 100,000 spatially explicit, photo-interpreted, attributed wetland polygons which are normally ideal for wetland class, form, and type classifications, but ultimately, these data are derived from a static interpretation of the landscape during late summer or fall. Therefore, the attribution of the water permanence of the interpreted wetland polygon typically will not match the permanence derived from EO data. Additionally, these wetland landscapes can change year-to-year and, therefore, the wetland landscape during the year of photo-interpretation may not resemble the one during the required year of classification. Dense, high-resolution, time-series photo-interpretation matching the years and seasons of the required EO data is the ideal training and validation data but, again, this is expensive and time-consuming. Time-series field observations of pothole wetlands over multiple years and seasons are also an option, but achieving a sufficient number of field sites to train modern machine learning algorithms is very challenging.

Despite these challenges, other studies have managed to map wetland potholes at smaller scales. For example, Wu et al. [24] managed to capture the temporal signature of pothole wetlands with multi-temporal National Agriculture Imagery Program (NAIP) imagery and a Light Detection and Ranging (LiDAR) Digital Elevation Model (DEM) using Google Earth Engine (GEE) [25] in North Dakota, United States. This proposed workflow is likely ideal for pothole mapping as it captured the natural seasonality and could map some of the smallest potholes with the 1 m resolution NAIP imagery. Unfortunately, NAIP is not available in Canada and, thus, another optical data source is needed. DeVries et al. [17] have also followed an optical multi-temporal approach for pothole mapping/monitoring in Saskatchewan, Canada using Landsat data. This method is promising for Canadian areas, but the authors acknowledged that future Sentinel-2 (S2) data will provide even better spatial and temporal resolutions for mapping small wetlands. In theory, Synthetic Aperture Radar (SAR) systems should provide the best data for capturing the hydrodynamics of pothole wetlands as SAR can detect open water and flooded vegetation with proper polarimetric configurations [26–28], and can provide a dense time-series data stack to capture all temporary and seasonal wetlands. Operationally, SAR does provide a few challenges. For instance, Sentinel-1 SAR provides weekly data for everywhere in the PPR,

but prior studies from DeLancey et al. [29] have shown poor performance of Sentinel-1 to distinguish seasonally flooded wetlands from native grasslands in the PPR of Alberta, Canada. More recent work by Schaffler et al. [30] applying Sentinel-1 SAR to multi-temporal water body detection in North Dakota, United States showed more promise, however. Other studies have used RADARSAT-2 to capture pothole/wetland hydrodynamics [31,32], but scaling up RADARSAT-2 workflows for large-scale inventory generation remains expensive and challenging. RADARSAT Constellation Mission (RCM) may be the next technological advancement in operational prairie pothole wetland mapping and monitoring, but a larger time-series stack is probably needed which is not currently available.

Knowing the limitations of traditional wetland classifications in the PPR and success of prior studies using multi-temporal EO data to capture hydrodynamics in the region, this study investigates the application of multi-temporal S2 data and GEE to map pothole wetland dynamics. We assessed how these time-series data can be used to produce a wetland inventory for areas in the PPR of Alberta, Canada. Specifically, we tested how hydroperiod data plus ancillary data could be used to generate an inventory at the CWCS class level and be further enhanced with water permanence from the AWCS wetland type level (Table 1). We also assessed a realistic minimum mapping unit (MMU) of these wetlands knowing that these features are typically very small. Our goal is to present a framework for operational mapping of PPR wetlands achieved with open-access EO data and no requirement of prior training and validation data.

2. Data and Methods

2.1. Study Area

The study area is located in the Grassland Natural Region of southern Alberta, Canada (area = 44,536 km^2), within the larger PPR of Canada and the United States (Figure 1). The Grassland region, often called prairie, is characterized by extensive grasses with shrubs in moist environments, and trees growing only along rivers [33]. The climate is continental semi-arid, with warm, dry summers and cool, dry winters [33]. The mean annual warmest and coldest month temperatures are 17.8 °C and −11.7 °C, respectively, whereas mean annual precipitation is 374 mm, with maximums typically occurring in June [33]. During our period of study, 2017–2020, the area experienced considerable drought conditions in summer 2017 and a higher-than-average snowpack in March and April of 2018 [34].

Prairie pothole wetlands within our study area occur in small (<1 ha), isolated, shallow depressions often <1 m [10], as they are throughout the PPR. Since they generally overlay glacial till with low water permeability and occur in a semiarid climate, their hydrology is largely dependent on precipitation, snowmelt, and evapotranspiration, which renders them highly dynamic [35]. These wetlands vary from temporary, where surface water is present only for a short time after heavy rain or spring snowmelt, to seasonal, where surface water lasts most but not all of a growing season, to semi-permanent or permanent, where surface water remains most or all of the year [8]. Temporary and seasonal wetlands are most abundant in our study area, and are particularly sensitive to climatic variability, climate change, and human modifications of the landscape [10]—e.g., ditches, drainage. A high annual variability in precipitation and evaporation rates leads to considerable variability in the number of water-filled basins within the PPR in any given season or year, changing with the occurrence of common drought and deluge climatic cycles [36].

Cultivation occurs throughout most of the area but is most prevalent in the northwest [33]. Other anthropogenic activities in this area include oil and gas developments, mines explorations, and feedlot operations [37]. For optimizing satellite data availability, the study area was processed as three sections (west, centre, and east) based on S2 orbital paths.

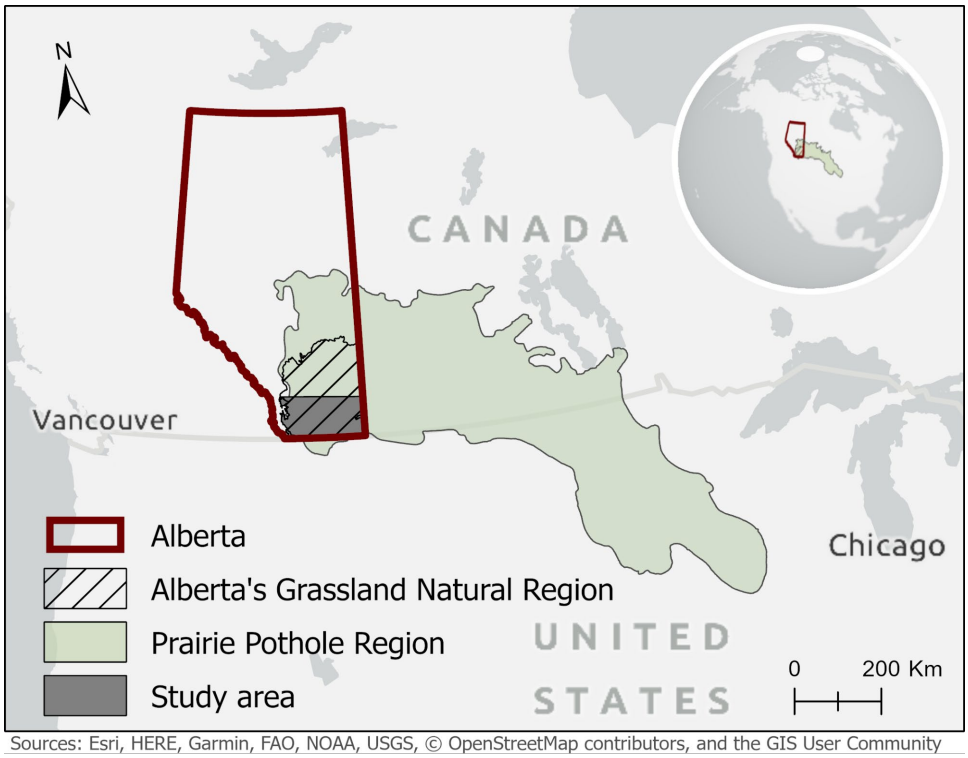

Figure 1. Study area located in the Grassland Natural Region of southern Alberta, Canada, and its coverage in the Prairie Pothole Region. Background is the Esri Light Gray Canvas baselayer [38]. (Sources: Esri, HERE, Garmin, FAO, NOAA, USGS, © OpenStreetMap contributors, and the GIS User Community).

2.2. Data

S2 imagery with minimal cloud, ice, and snow cover acquired between April and October 2017–2020 were selected and processed in GEE [25]. Over the entire study area, 36 S2 image dates (representing 233 S2 image tiles) were utilized. These comprised 13–15 images per processing section, of which 3 represented spring conditions, 3–4 represented summer conditions, and 7–8 represented fall conditions. Harnessing seasonal imagery for hydroperiod calculation captures temporary wetlands, typically found in spring, as well as semi-permanent wetlands found well into dry seasons (Figure 2).

An Advanced Land-Observing Satellite (ALOS) DEM and topographic derivatives, specifically Topographic Wetness Index (TWI) [12], was applied in the post-processing quality control phase to exclude false flooded areas on slopes due to shadows in times with lower sun angles (i.e., April and October). The 2018 Human Footprint Inventory layer developed by the ABMI [37] was also used to exclude human built-up features, including roads, railways, verges, mines, industrial areas, landfills, wind generation areas, confined feeding operations, and forest harvest areas. Finally, a 30 m forest Canopy Height Model (CHM) based on 2019 Global Ecosystem Dynamics Investigation (GEDI) spaceborne LiDAR transects extrapolated with Landsat data [39] was used to separate the marsh (graminoid) and swamp (shrub and tree) classes. On a global basis, this product has been evaluated as 88% accurate at separating forest (>3 m trees) from non-forest compared to airborne LiDAR validation data [39].

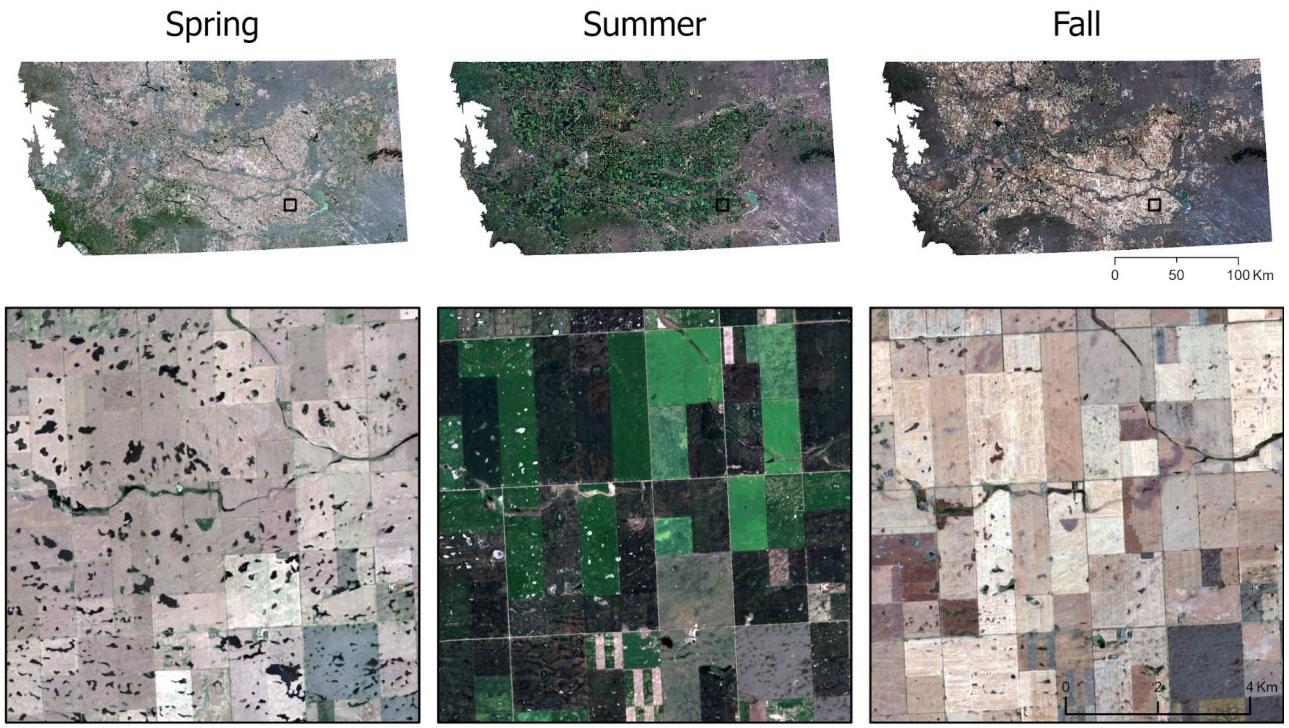

Figure 2. S2 RGB mosaics for spring (2018), summer (2020), and fall (2020) with a zoomed map inset showcasing seasonal flood dynamics of prairie potholes.

2.3. Hydroperiod

Flooded/non-flooded training data were created by labelling segments in three S2 image dates (spring, summer, and fall). First, a Simple Non-Iterative Clustering (SNIC) [40] algorithm was applied to 10 m resolution bands of the S2 imagery in GEE. In GEE, the size of segmented objects varies dynamically as a user zooms in and out to smaller or larger map viewing scales and different pyramiding levels are applied to the imagery; to fix the segments to a set size, a scale is specified in the export operation. This is not to be confused with the spatial resolution of the input data. For the prairie pothole wetlands, a relatively fine export scale was desired to capture as many small features as possible. By trial and experimentation, it was determined that a nominal scale (zoom level) of 2 m/pixel, in combination with an initial seed location spacing of 36 pixels and a compactness value of 0.1, produced segments that best represented the size and shape of wetland features in this area. These segments varied in size from a theoretical minimum of 2 m^2 to over 30,000 m^2 with a mean around 2000 m^2. Segment size is determined by the heterogeneity of pixel values in a given area. The initial SNIC segments were further refined by merging spectrally similar neighboring segments based on bands 4 (red), 8 (NIR), 11, and 12 (SWIR) at a weighting ratio of 1:3:2:3, and then exported as polygons.

With reference to the representative seasonal S2 images and ESRI basemap imagery, a set of the merged segment polygons were labeled as flooded or non-flooded by a photo-interpreter. Within a given section, each seasonal training datum had a total of roughly 400 labelled polygons, of which approximately 50% were flooded and 50% were non-flooded.

Flooded/non-flooded classification was performed on a date-by-date basis for selected S2 images of each processing section using the merged segments in a Random Forest (RF) classifier [41]. Each S2 image was segmented via the merged SNIC algorithm in GEE using the 10 m resolution bands: 2 (blue), 3 (green), 4 (red), and 8 (NIR). For each segment, the mean and standard deviation were calculated for the S2 10 m bands and the 20 m bands (5–7 (vegetation red edge), 11, and 12 (SWIR)), as well as the perimeter, width, height, and area of the segments. These segment statistics, along with the flooded/non-flooded labels, were inputs for the RF classifier, which was trained on 5000 pixels using 50 decision trees.

Finally, the results (i.e., flooded/non-flooded binary rasters) were exported from GEE again at a 2 m scale to achieve the smallest MMU possible, which typically produced 400–800 m^2 wetland segments.

Exported flooded/non-flooded binary rasters were quality controlled by applying TWI [12] and human footprint [37] masks, as well as manually removing some falsely flooded pixels. To calculate hydroperiod for each section, all binary flooded/non-flooded rasters were added together, divided by the total number of images per section, and multiplied by 100 to derive the frequency of flooding as a percentage.

2.4. Wetland Inventory

To generate a wetland inventory product, the hydroperiod data were first divided into five classes: (1) permanent open water, (2) semi-permanent wetland, (3) seasonal wetland, (4) temporary wetland, and (5) upland (i.e., non-wetlands). These classes were divided according to a set of thresholds (Table 2). Subsequently, wetland areas were divided into marsh and swamp classes given that >99% of wetlands in this area are marsh and swamp. The major separator for these classes is vegetation (i.e., graminoid marsh versus shrub or treed swamp). Therefore, the GEDI-based CHM was used to distinguish marsh and swamp. Any wetland polygon under 2 m mean vegetation height was considered to be graminoid marsh and anything above 2 m was considered a shrubby or treed swamp. The end result of this rule-based classification is a seven-class wetland inventory product.

Table 2. Rules used for dividing wetland classes according to hydroperiod and vegetation height data.

Hydroperiod Value (%)	Vegetation Height (m)	Wetland Classification
85–100	Not applied	Open water
51–84	<2	Semi-permanent marsh
51–84	>2	Semi-permanent swamp
20–50	<2	Seasonal marsh
20–50	>2	Seasonal swamp
1–19	<2	Temporary marsh
1–19	>2	Temporary swamp
0–1	Not applied	Upland

2.5. Accuracy Assessment

The wetland inventory product was validated with independent photo-interpreted data from DUC, which included both Canadian Wetland Inventory (CWI) data, and other similar DUC datasets overlapping our study area. The CWI data cover some northern portions of our study area, are dated to 2015, and provided information at the wetland class level (Table 1). Other DUC data were interpreted using multispectral aerial photos (i.e., visible and near-infrared) from August 2018 over a set of 5 × 5 km^2 blocks in the area surrounding Pakowki Lake in the southern portion of our study area, and provided wetland class information (Table 1). Accuracy was mainly assessed via user, producer, and overall accuracies using the area of the CWCS wetland classes, due to limited information on water permanence. That is, accuracies of open water, marsh, swamp, and upland classes (as well as wetland vs. upland) were assessed by overlaying our wetland inventory with these validation datasets to extract areas of agreement and disagreement between different classes.

Datasets for comparing with and validating the hydroperiod data, which underlies our wetland inventory, do not currently exist for our study area and hinder our ability to independently assess those data's accuracy. Nevertheless, a single flooded/non-flooded binary raster from spring 2018 was used as a partial assessment of hydroperiod accuracy by holding back 20% of the manually-labeled segments as validation segments (i.e., these

were excluded from training), in a quick assessment of hydroperiod accuracy using the same spatial overlay approach.

3. Results

Our 2017–2020 hydroperiod product for the study area captured wetlands down to a minimum area of 400 m^2 and a flood frequency ranging from 1–100% (Figure 3). Flooded areas covered 2600 km^2, with nearly 70% of that coverage constituting infrequent flooding (i.e., flood frequency of 1–20%). In comparison, moderate (21–80%) and high (81–100%) flood frequency classes covered 478 km^2 and 367 km^2, respectively. The quick assessment of the hydroperiod with the set of withheld labeled validation segments from a spring 2018 flooded/non-flooded classification showed 95% accuracy in classifying flooded and non-flooded segments.

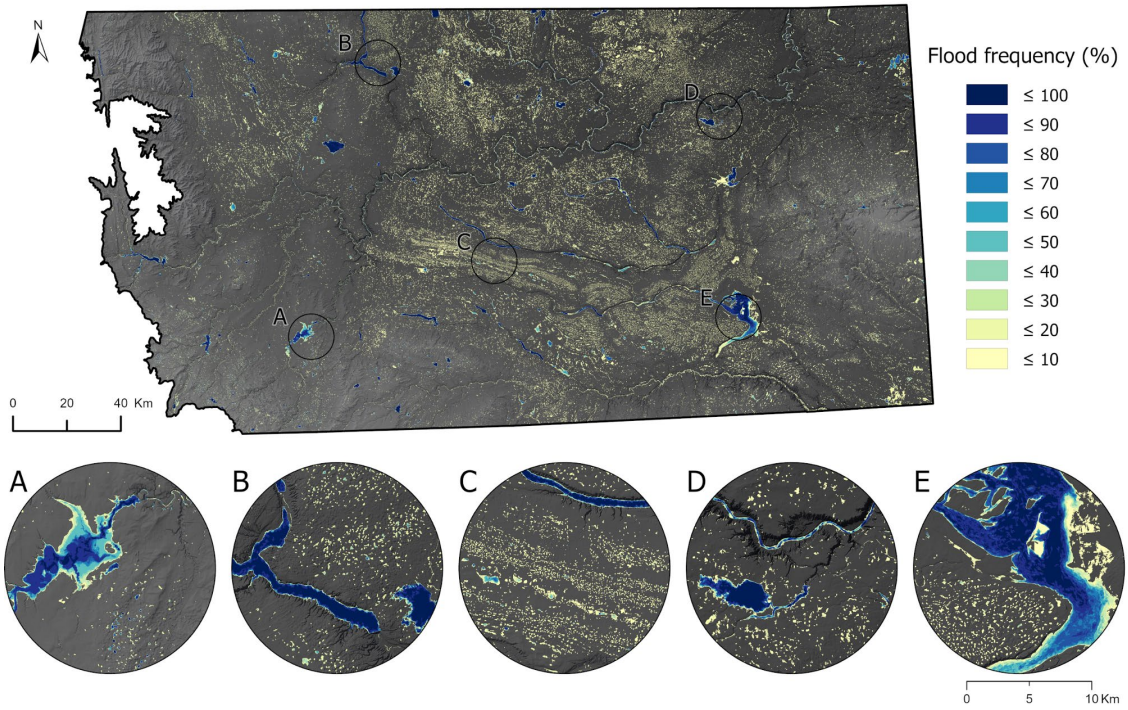

Figure 3. The hydroperiod for 2017–2020 showing flood frequency (%) classes from 1–100%. Circled map insets (**A**–**E**) show select magnified regions. Background is a DEM-derived hillshade.

When converting the hydroperiod data to inventory data (Figure 4), it was observed that the landscape was primarily dominated by temporary and seasonal marshes. Swamps are present but usually in small numbers and are more commonly found in the western portions of the study area closer to the Rocky Mountains. Semi-permanent wetlands are typically larger depressions which only dry out in dry periods during fall, while temporary and seasonal wetlands are numerous and typically small. A detailed view of the results in a cultivated area that contained distinct potholes with varying permanence highlights the dynamic nature of these wetland features (Figure 5). Semi-permanent marsh is the largest and currently flooded in the ESRI baselayer imagery. Seasonal wetlands are moderate in size and show flooded or saturated wetland vegetation. Temporary wetlands are the smallest and, in some cases, appear to be normal agricultural fields in the ESRI imagery. These are the wetlands that likely exist for only a few weeks to a month in some seasons.

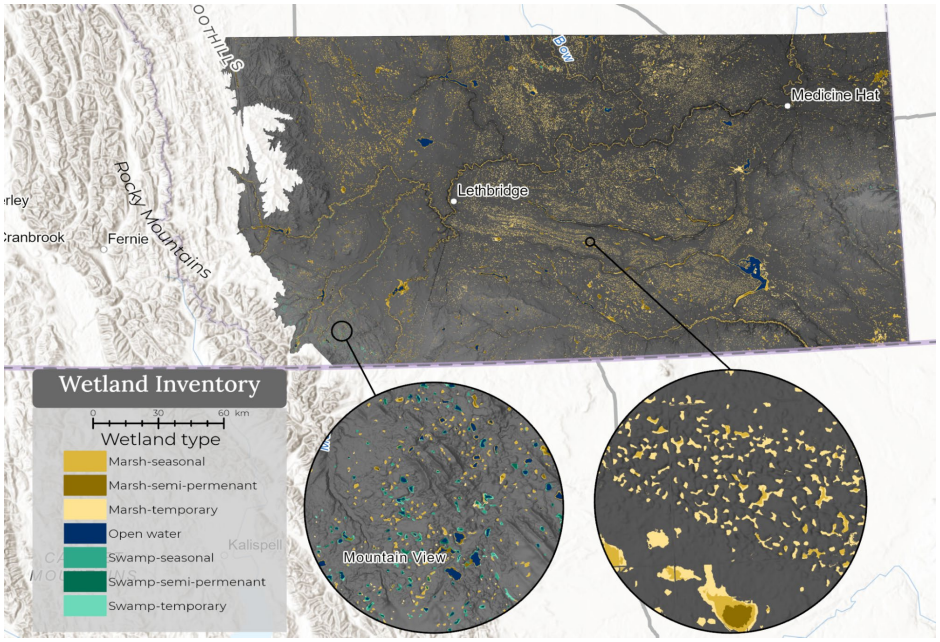

Figure 4. The seven-class wetland inventory for the study area. Two insets show areas with different wetland classes and permanence. Background is the Esri Terrain with Labels baselayer [42]. (Sources: Esri, HERE, Garmin, FAO, NOAA, USGS, © OpenStreetMap contributors, and the GIS User Community).

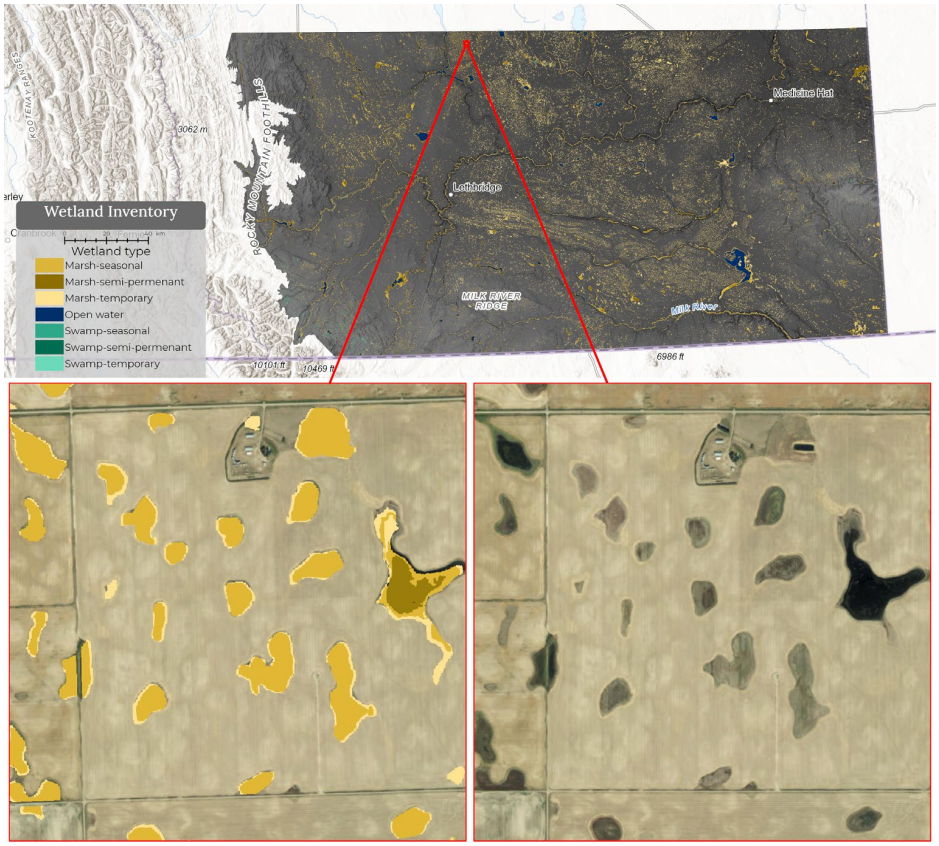

Figure 5. Close-up view of a section of the wetland inventory product with comparison to the Esri World Imagery baselayer [43] (ESRI Canada, HERE, Garmin, NOAA, USGS, EPA, NRCAN, Parks Canada, CGIAR, Vulcan County, Maxar). The three levels of marsh permanence can be seen in this one area.

For a comparison of our wetland inventory product, the photo-interpreted DUC validation datasets revealed that non-wetland areas had a very high accuracy (98%) in assessments at both the class and the wetland/non-wetland level (Tables 3 and 4). The marsh class showed a 60% user and 72% producer accuracy compared to the DUC data with the most confusion occurring with upland. The open water class achieved close to 100% user accuracy but only 9% producer accuracy, with most of shallow/open water in the DUC data being classified as marsh. The small area of swamp in the DUC data did not match up with the wetland inventory product, suggesting these data are insufficient for assessing the accuracy of the swamp class. Overall, the wetland inventory product was assessed to be have 96% accuracy at the wetland/upland level, although most of this accuracy comes from the relative area of the upland class.

Table 3. Accuracy assessment of the wetland inventory product. Validation data are from photo interpretation data by Ducks Unlimited Canada (DUC). Numbers are the area of each class in hectares (OA: Overall Accuracy).

	Hydroperiod-Based Wetland Inventory					
Validation Dataset	**Marsh**	**Open Water**	**Swamp**	**Upland**	**Total**	**Producer Accuracy**
Marsh	2260.33	0.04	0.58	878	3138.95	0.72
Shallow Open water	616.24	66.67	1.19	42.31	726.41	0.09
Swamp				0.1	0.1	
Upland	903.62		0.09	45,225.74	46,129.45	0.98
Total	3780.19	66.71	1.86	46,146.15		
User Accuracy	0.6	1		0.98		OA = 95%

Table 4. Accuracy assessment of the wetland inventory product, summarized at the wetland/upland level, using the same validation data as in Table 3. Numbers are the area of each class in hectares (OA: Overall Accuracy).

	Hydroperiod-Based Wetland Inventory			
Validation Dataset	**Wetland**	**Upland**	**Total**	**Producer Accuracy**
Wetland	2945.05	920.41	3865.46	0.76
Upland	903.71	45,225.74	46,129.45	0.98
Total	3848.76	46,146.15		
User Accuracy	0.77	0.98		OA = 96%

4. Discussion

The S2-derived hydroperiod was able to capture wetland flooding dynamics of PPR wetlands in our study area down to 400–800 m^2. Capturing these smaller potholes was achieved by running the segmentation classifications at a 2 m resolution, which captured pothole shapes better than if it were run at a coarser scale. However, it is likely that closer spacing of the segmentation at larger scales (5 m) can also achieve a similar MMU. It is also possible that an unsupervised pixel-based classification followed by a segmentation could achieve a better MMU. Individual flooded/non-flooded classifications had about 95% overall accuracy which we would expect to be similar across most S2 images, but it would be very difficult to validate all time-series classifications. The hydroperiod results show this area is incredibly dynamic with very few areas actually having permanent open water and many potholes which experienced very infrequent flooding events. Most of the peak flooding images came from spring 2018 which was likely due to the large snowpack that occurred in March and April 2018 [34].

The timing of cloud-free S2 images with peak flooding can greatly affect the hydroperiod results. There does appear to be a faint visible seam in the hydroperiod data (Figure 3) which lines up with the boundary between the west and center S2 section orbits. The center orbit appears to have captured peak flooding on 24 April 2018, while the west orbit had images slightly later in the year. For this reason, the center orbit does have a few more temporary wetlands. This is a limitation of the S2 data because cloud-free images during the ideal peak flooding times in spring are not always available.

It is not clear if the S2 hydroperiod data captures sub-vegetation flooding dynamics. The binary classifications do classify dark/saturated vegetated wetlands as flooded, but it is likely that SAR coherence products or polarimetric data with longer wavelengths (e.g., L-band) are needed to capture these sub-vegetation/-canopy water dynamics. Fortunately, the vast majority of wetlands in this area are open and, thus, flooding is visible to optical sensors. Overall, S2 hydroperiod accurately and effectively captured water dynamics in the PPR and most limitations are from the availability of cloud-free S2 post snow melt in early spring.

Theoretically, SAR data should be ideal for capturing these pothole water dynamics [27,31,32]. Similar hydroperiod products could be obtained by thresholding SAR backscatter to capture open water in wetland areas. While Schaffler et al. [30] encountered some success in mapping surface water dynamics with Sentinel-1 SAR image time series in South Dakota, prior research in Alberta by DeLancey et al. [29] has shown Sentinel-1 SAR had little value for differentiating open water and grasslands in southern Alberta due to the lower noise floor of Sentinel-1. Other sensors such as RADARSAT-2 seem to be valuable for water dynamics in the PPR [31] but prove to be much harder to apply operationally over larger areas. SAR data will likely be very important for future efforts at PPR wetland mapping/monitoring but S2 data seem to be the best open-access data, currently, for capturing water dynamics and achieving a relatively small MMU.

The resulting wetland inventory product generated from the hydroperiod data plus GEDI-based CHM for marsh versus swamp proved to be accurate at the wetland class level when compared to photo-interpreted data from DUC. Unsurprisingly, upland (i.e., non-wetlands) were very accurate (98%) as this method only classified wetlands if the area, at any time, was flooded/saturated during the S2 image stack. The producer and user accuracies of the marsh class (73% and 60%, respectively) were considered reasonably accurate given the small and dynamic nature of this landcover type. The majority of both the omission and commission errors in the marsh class is the result of confusion with upland, and there does not appear to be a systemic bias in either direction. Some of this discrepancy is probably due to what a photo-interpreter observed and delineated in the high-resolution imagery at a particular point in time and what was recorded and resolved by the time-series S2 data, for our classification. As noted, several physical and ecological components of the PPR landscape can appear very different from year to year and season to season, given that the majority of the wetland features we identified are temporary marshes with hydroperiods of 20% and below. As a result, we argue that accuracy measurements for this area are useful but do not tell the whole story of how the data are capturing ecological patterns. A mismatch in results is influenced by both the scale and the timing of the input data versus validation data. The swamp class could not be reliably assessed in this study due to limited samples in the assessment area. Swamps are more prevalent farther west towards the Rocky Mountains, where accuracies may be higher, but we did not have access to validation data from this area.

The 9% producer accuracy of the open water hydroperiod class requires some explanation. Open water as defined by the hydroperiod method included all areas flooded 85% or more of the time. This includes deep water bodies like reservoirs and lakes, which comprises most of the permanent open water area in the hydroperiod-based inventory, as well as shallow open water wetlands. The validation data from DUC focused on shallow open water wetlands only, however, and thus does not include of the obvious large water bodies. This is an important source of misalignment with this validation dataset. Whereas nearly all the open water in the our hydroperiod-based inventory corresponded to shallow open water in the validation dataset, generating almost 100% user accuracy, a significant amount of shallow open water in the validation data was classified as marsh by the hydroperiod method. These shallow open water wetlands likely appeared dry in two or more of the S2 image dates, resulting in less than 85% hydroperiod calculation from the image stack, and subsequent placement in the marsh class using this approach. They were evidently filled with open water at the time of the DUC air photo acquisition, however, and captured as such in the validation data. There is clearly some scope for overlap in the open water and marsh classes as both can be seasonal or semi-permanent in nature, and this validation discrepancy highlights a subset of features (temporary, seasonal, or semi-permanent shallow open water wetlands are captured quite differently on the basis of a hydroperiod rather than a single image date. A possible solution could be to distinguish shallow open water from graminoid marsh using optical vegetation productivity measures (e.g., Normalized Difference Vegetation Index (NDVI)). This approach requires further study. We were not able to validate the water permanence classes as this would require consistent field monitoring of wetlands. However, visual assessment (Figure 5) shows that class permanence matches with what we would expect ecologically. Temporary wetlands are small and barely visible in summer/fall high-resolution imagery (often plowed over in agricultural areas). Seasonal wetlands are visible vegetated depressions in the landscape and semi-permanent wetlands that are larger and usually have open water.

The major finding of this work is that classifying water frequently and through time can generate accurate and reliable wetland data in the PPR and, potentially, other wetland landscapes with open vegetation structures (maybe wetland landscapes seen in studies like Hardy et al. [44]). Here, we have illustrated the advantages of multi-seasonal S2 optical imagery, aligning well with recommendations provided by Montgomery et al. [10] in their review. However, it is likely that at least four years of time-series data are needed because "peak wetland flooding" does not always line up with cloud-free S2 image dates. GEE or other cloud computing platforms are probably needed to make this workflow efficient as processing thousands of S2 images and the classification of water in these images is a computationally intensive process. Spring 2018 images were very important for these areas as most of the temporary wetlands were detected with this imagery. Without these images, the majority of temporary wetlands would be missed. These "peak wetland flooding" images are key to this workflow because these images essentially act as a high resolution, hydrologically corrected DEM. After snow melt, all topographic lows (potholes) will naturally fill with water and thus mapping pothole depressions is essentially a water classification exercise, which is well established in the remote sensing literature [45]. It is important to note, however, that while these peak flooding spring images are integral to capturing temporary wetlands, it is the long time-series of multiple images from different periods that enable us to distinguish temporary, seasonal, semi-permanent, and permanent wetlands from one another (Table 2; Figure 5). The combination of images provides us with information on hydroperiod or frequency of flooding over time.

In this workflow, there is no need for complicated convolutional neural networks [15], multi-class multi-sensor models, or high-density LiDAR point clouds. These methods are valuable and will likely produce comparable results but they will be much more time- and labor-intensive and, in our experience, without careful calibration of training data, they can often produce odd predictions.

Another major finding of this work is that field or photo-interpretation may not be needed to generate reliable wetland data in the PPR. With open-access EO data and open processing platforms (e.g., GEE), the most expensive part of large-scale landcover mapping is often field data or high-resolution photo-interpretation data needed for training and validation of models. This method proposes a quick self-labeling of flooded and non-flooded areas from S2 images in three distinct seasons as necessary training data. Some independent validation data will always be required but this can be at a smaller scale than a normal dataset for training and validation. This method also proves to be highly scalable. Similar methods have been employed to complete a wetland inventory in the Prairie region of Alberta [46] and future applications of this work are planned in the PPR areas of Saskatchewan.

Despite improvements to mapping potholes using the workflow presented, its simplicity does come with limitations. The biggest being its strong dependency on the timing of cloud-free S2 images in alignment with key wetland seasonal states (peak flooding, green up, and dry season). This workflow also depends on seasonal snow melt although the methods could potentially be of use to areas that have other reliable wetland flooding seasonal dynamics (i.e., very wet and very dry seasons). This method also cannot provide information about wetland form and vegetation structure because wetlands are only classified through the presence of seasonal water and modelled vegetation height. Additionally, in a complex wetland environment with many more wetland types and forms (bogs and fens), this method will fail to differentiate these classes. Therefore, the methods presented here are probably best served for large-scale wetland inventory data across PPR areas in Canada and the United States.

Moving forward, various technological improvements can help the classification of water across time and, thus, improve PPR wetland data. The RCM and NASA-ISRO Synthetic Aperture Radar (NISAR) should provide better SAR data to monitor open water and wetland flooding across time. These SAR datasets can hopefully provide additional wetland dynamic information, such as open water flood frequency (via specular scattering) and flooded vegetation frequency (via double-bounce scattering) [27]. Additionally, optical datasets tend to move towards higher-resolution images with more frequent revisit times, which will help capture small and temporary wetland features. S2 10 m resolution images and the satellite's five-day revisit time are already generally sufficient for the application of PPR wetland mapping, but many temporary wetlands are still missed with a 400–800 m^2 MMU.

Results of this study are comparable to those found in other, similar research. For instance, Wu et al. [24] presented comparable results by focusing on wetland dynamics in a PPR area in the United States. Our study substitutes S2 data in GEE to capture pothole dynamics rather than NAIP imagery, which is only available for the United States. DeVries et al. [17] also achieved similar results in the Saskatchewan PPR with Landsat data and an unsupervised sub-pixel water fraction. As DeVries et al. [17] note, it is likely that the S2 methods here improve upon this work by providing higher spatial and temporal resolution when compared to Landsat. Like this study, Montgomery et al. [31] found very few areas of semi-permanent and permanent wetlands with most potholes being temporary and seasonal. When compared to other existing inventories in Alberta, results from this study typically show many more wetland features (Figure 6). When compared to the SPOT-derived portions of Alberta's Merged Wetland Inventory (Figure 6b), the time-series-based results (Figure 6a) show about 8–10 times more pothole wetland features, likely due to the use of early spring "peak flooding" imagery. Comparisons to inventories from high-resolution photo-interpretation data (see Table 4 validation) show comparable results, although the photo-interpreted inventories capture many more wetlands that are smaller than 400 m^2 and are generally more reliable.

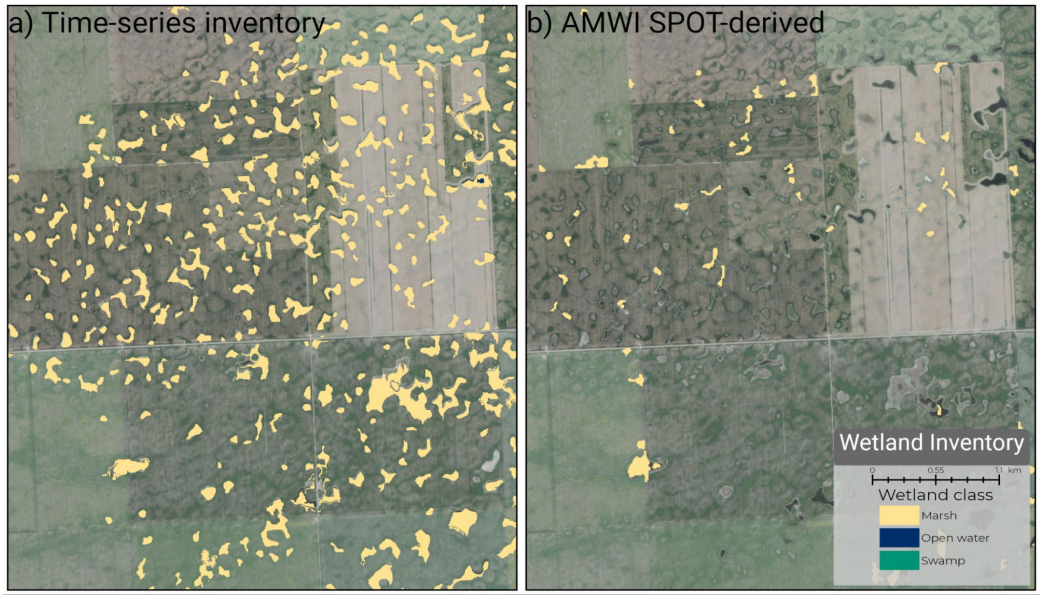

Figure 6. Comparison between (**a**) the time-series-based inventory for this study, and (**b**) the SPOT-derived Alberta Merged Wetland Inventory for an area with significant amounts of seasonal and temporary pothole wetlands. Background is the Esri World Imagery baselayer [43] (Source: Forty Mile County No. 8, Village of Warner, Maxar).

5. Conclusions

The PPR is a unique ecological region with wetland features that are both ecologically and economically important. These wetland potholes are difficult to map/inventory for conservation purposes because they are very dynamic seasonally and annually. It is also hard to collect proper field training and validation data for classification models. Past studies have found success using large satellite image stacks to capture the temporal signature of these wetland potholes. This study recreated some of these methods with 2017–2020 S2 data processed in GEE. By classifying water/flooding through time with a fine 2 m scale segmentation in GEE, we captured the hydroperiod (flood frequency) of pothole wetlands down to a MMU of 400 m^2. We used this hydroperiod data along with the GEDI CHM data to generate a seven-class wetland inventory. Wetland permanence was defined with the hydroperiod data, and swamp versus marsh classes were defined by the GEDI CHM. This relatively simple classification showed an overall accuracy of 95%, which is driven mainly by the ratio of upland to wetland areas, while wetland user and producer accuracies were approximately 70%. Shallow open water had a producer accuracy of only 9% due to commission errors with marshes, suggesting that some shallow open water overlapped with marshland in water permanence and is captured differently using our hydroperiod approach versus the photo-interpretation used in the validation data. The hydroperiod method does still have limitations as it is optimized for regions with open vegetation structures, reliable seasonal flooding, and non-complex wetland types. When compared to other existing remote sensing-derived inventories in the area, this method classifies many more pothole wetland features, indicating the power of dense time-series data to capture temporary pothole wetlands.

Overall, we found that classifying water/flooding across four or more years with S2 data can generate a reliable wetland inventory in the PPR. We also found that a minimum of 8–10 satellite image dates are likely needed to accurately capture all wetland areas in the PPR and that early spring images (post snow melt) are probably the most important for identifying temporary pothole wetlands. Finally, we suggest that normal landcover or wetland training data may not be needed to generate wetland inventories in the PPR. We observed that simple, self-labelling of flooding and not flooded segments in S2 images is all that is needed to classify water across time.

We hope that methods similar to this can be scaled up to large areas of the PPR to produce a reliable inventory of the small but valuable wetland features. Monitoring of these features can then simply be done through the tracking of their seasonal flooding dynamics. Moving forward, EO data will only improve for tracking wetland flooding through time with better SAR sensors and higher-resolution optical sensors. An accurate baseline inventory of these PPR wetland features will help with the conservation of pothole wetlands, thus preserving their ecosystem functions and the valuable habitat for various species.

Author Contributions: Conceptualization, E.R.D.; methodology, E.R.D., A.C., L.B., F.G., M.A. and B.B.; software, E.R.D. and A.C.; formal analysis, E.R.D. and A.C.; writing—original draft preparation, E.R.D. and A.C.; writing—review and editing, L.B., F.G., M.A., B.B., J.K. and J.N.H.; visualization, E.R.D. and A.C.; project administration, J.K.; funding acquisition, J.K. All authors have read and agreed to the published version of the manuscript.

Funding: This research was funded by Alberta Environment and Parks, Government of Alberta, Canada, grant number 20GRPOL10.

Data Availability Statement: The data produced in this study have been incorporated into the publicly available ABMI Wetland Inventory dataset, which can be found here: https://abmi.ca/home/data-analytics/da-top/da-product-overview/Advanced-Landcover-Prediction-and-Habitat-Assessment--ALPHA--Products/ABMI-Wetland-Inventory.html, accessed on 26 May 2022.

Acknowledgments: Validation data were provided by the Ducks Unlimited Canada Prairie Wetland Mapping Unit. Maps were created using Esri's ArcGIS software and some Esri baselayers (see References).

Conflicts of Interest: The authors declare no conflict of interest. The funders had no role in the design of the study; in the collection, analyses, or interpretation of data; in the writing of the manuscript, or in the decision to publish the results.

References

1. Batt, B.; Anderson, M.; Anderson, C.; Caswell, F. The Use of Prairie Potholes by North American Ducks. In *Northern Prairie Wetlands*; van der Valke, A., Ed.; Iowa State University Press: Ames, IA, USA, 1989; Volume 204, p. 227.
2. Pattison-Williams, J.K.; Pomeroy, J.W.; Badiou, P.; Gabor, S. Wetlands, flood control and ecosystem services in the Smith Creek Drainage Basin: A case study in Saskatchewan, Canada. *Ecol. Econ.* **2018**, *147*, 36–47. [CrossRef]
3. Wu, Q.; Lane, C.R. Delineation and quantification of wetland depressions in the Prairie Pothole Region of North Dakota. *Wetlands* **2016**, *36*, 215–227. [CrossRef]
4. Wu, Q.; Lane, C.R.; Wang, L.; Vanderhoof, M.K.; Christensen, J.R.; Liu, H. Efficient delineation of nested depression hierarchy in digital elevation models for hydrological analysis using level-set method. *J. Am. Water Resour. Assoc.* **2019**, *55*, 354–368. [CrossRef] [PubMed]
5. Dahl, T.E. *Wetlands Losses in the United States, 1780's to 1980's*; US Department of the Interior, Fish and Wildlife Service: Washington, DC, USA, 1990.
6. Brinson, M.M.; Malvárez, A.I. Temperate freshwater wetlands: Types, status, and threats. *Environ. Conserv.* **2002**, *28*, 115–133. [CrossRef]
7. Warner, B.; Rubec, C. *The Canadian Wetland Classification System*; Wetlands Research Centre, University of Waterloo: Waterloo, ON, Canada, 1997.
8. Water Policy Branch, Policy and Planning Division. Alberta Environment and Sustainable Resource Development. In *Alberta Wetland Classification System*; Water Policy Branch, Policy and Planning Division: Edmonton, AB, Canada, 2015.
9. Stewart, R.E.; Kantrud, H.A. *Classification of Natural Ponds and Lakes in the Glaciated Prairie Region*; U.S. Bureau of Sport Fisheries and Wildlife: Washington, DC, USA, 1971; Volume 92.
10. Montgomery, J.S.; Mahoney, C.; Brisco, B.; Boychuk, L.; Cobbaert, D.; Hopkinson, C. Remote Sensing of Wetlands in the Prairie Pothole Region of North America. *Remote Sens.* **2021**, *13*, 3878. [CrossRef]
11. Boudart, J. Mapping the Way for Conservation: Using Cutting-Edge Geographic Information Systems Technology, Ducks Unlimited Is Harnessing the Power of Data to Guide Its Work. Available online: https://www.ducks.org/conservation/national/mapping-the-way-for-conservation (accessed on 23 May 2022).
12. Hird, J.N.; DeLancey, E.R.; McDermid, G.J.; Kariyeva, J. Google earth engine, open-access satellite data, and machine learning in support of large-area probabilistic wetland mapping. *Remote Sens.* **2017**, *9*, 1315. [CrossRef]
13. Amani, M.; Mahdavi, S.; Afshar, M.; Brisco, B.; Huang, W.; Mirzadeh, S.M.J.; White, L.; Banks, S.; Montgomery, J.; Hopkinson, C. Canadian wetland inventory using google earth engine: The first map and preliminary results. *Remote Sens.* **2019**, *11*, 842. [CrossRef]

14. Merchant, M.A.; Warren, R.K.; Edwards, R.; Kenyon, J.K. An object-based assessment of multi-wavelength SAR, optical imagery and topographical datasets for operational wetland mapping in boreal Yukon, Canada. *Can. J. Remote Sens.* **2019**, *45*, 308–332. [CrossRef]
15. DeLancey, E.R.; Simms, J.F.; Mahdianpari, M.; Brisco, B.; Mahoney, C.; Kariyeva, J. Comparing deep learning and shallow learning for large-scale wetland classification in Alberta, Canada. *Remote Sens.* **2020**, *12*, 2. [CrossRef]
16. Mahdianpari, M.; Salehi, B.; Mohammadimanesh, F.; Brisco, B.; Homayouni, S.; Gill, E.; DeLancey, E.R.; Bourgeau-Chavez, L. Big data for a big country: The first generation of Canadian wetland inventory map at a spatial resolution of 10-m using Sentinel-1 and Sentinel-2 data on the Google Earth Engine cloud computing platform. *Can. J. Remote Sens.* **2020**, *46*, 15–33. [CrossRef]
17. DeVries, B.; Huang, C.; Lang, M.W.; Jones, J.W.; Huang, W.; Creed, I.F.; Carroll, M.L. Automated quantification of surface water inundation in wetlands using optical satellite imagery. *Remote Sens.* **2017**, *9*, 807. [CrossRef]
18. Alberta Biodiversity Monitoring Institute. *ABMI 3x7 Photoplot Landcover Dataset Data Model*; Alberta Biodiversity Monitoring Institute: Edmonton, AB, Canada, 2016; p. 69.
19. Castilla, G.; Hird, J.; Hall, R.J.; Schieck, J.; McDermid, G.J. Completion and updating of a landsat-based land cover polygon layer for Alberta, Canada. *Can. J. Remote Sens.* **2014**, *40*, 92–109. [CrossRef]
20. DeLancey, E.R.; Kariyeva, J.; Bried, J.T.; Hird, J.N. Large-scale probabilistic identification of boreal peatlands using Google Earth Engine, open-access satellite data, and machine learning. *PLoS ONE* **2019**, *14*, e0218165. [CrossRef] [PubMed]
21. Pouliot, D.; Latifovic, R.; Pasher, J.; Duffe, J. Assessment of convolution neural networks for wetland mapping with landsat in the central Canadian boreal forest region. *Remote Sens.* **2019**, *11*, 772. [CrossRef]
22. Amani, M.; Brisco, B.; Mahdavi, S.; Ghorbanian, A.; Moghimi, A.; Delancey, E.; Merchant, M.A.; Jahncke, R.; Fedorchuk, L.; Mui, A. Evaluation of the Landsat-based Canadian Wetland Inventory Map using Multiple Sources: Challenges of Large-scale Wetland Classification using Remote Sensing. *IEEE J. Sel. Top. Appl. Earth Obs. Remote Sens.* **2020**, *14*, 32–52. [CrossRef]
23. Amani, M.; Poncos, V.; Brisco, B.; Foroughnia, F.; DeLancey, E.D.; Ranjbar, S. InSAR Coherence Analysis for Wetlands in Alberta, Canada Using Time-Series Sentinel-1 Data. *Remote Sens.* **2021**, *13*, 3315. [CrossRef]
24. Wu, Q.; Lane, C.R.; Li, X.; Zhao, K.; Zhou, Y.; Clinton, N.; DeVries, B.; Golden, H.E.; Lang, M.W. Integrating LiDAR data and multi-temporal aerial imagery to map wetland inundation dynamics using Google Earth Engine. *Remote Sens. Environ.* **2019**, *228*, 1–13. [CrossRef]
25. Gorelick, N.; Hancher, M.; Dixon, M.; Ilyushchenko, S.; Thau, D.; Moore, R. Google Earth Engine: Planetary-scale geospatial analysis for everyone. *Remote Sens. Environ.* **2017**, *202*, 18–27. [CrossRef]
26. Brisco, B.; Schmitt, A.; Murnaghan, K.; Kaya, S.; Roth, A. SAR polarimetric change detection for flooded vegetation. *Int. J. Digit. Earth* **2013**, *6*, 103–114. [CrossRef]
27. Brisco, B. Mapping and Monitoring Surface Water and Wetlands with Synthetic Aperture radar. In *Remote Sensing of Wetlands: Applications and Advances*; Tiner, R.W., Lang, M.W., Klemas, V.V., Eds.; CRC Press, Taylor & Francis Group: Boca Raton, FL, USA, 2015; pp. 119–136.
28. White, L.; Brisco, B.; Dabboor, M.; Schmitt, A.; Pratt, A. A collection of SAR methodologies for monitoring wetlands. *Remote Sens.* **2015**, *7*, 7615–7645. [CrossRef]
29. DeLancey, E.R.; Kariyeva, J.; Cranston, J.; Brisco, B. Monitoring hydro temporal variability in Alberta, Canada with multi-temporal Sentinel-1 SAR data. *Can. J. Remote Sens.* **2018**, *44*, 1–10. [CrossRef]
30. Schaffler, S.; Chini, M.; Dorigo, W.; Plank, S. Monitoring surface water dynamics in the Prairie Pothole Region of North Dakota using dual-polarised Sentinel-1 synthetic aperture radar (SAR) time series. *Hydrol. Earth Syst. Sci.* **2022**, *26*, 841–860. [CrossRef]
31. Montgomery, J.S.; Hopkinson, C.; Brisco, B.; Patterson, S.; Rood, S.B. Wetland hydroperiod classification in the western prairies using multitemporal synthetic aperture radar. *Hydrol. Process.* **2018**, *32*, 1476–1490. [CrossRef]
32. DeLancey, E.R.; Brisco, B.; Canisius, F.; Murnaghan, K.; Beaudette, L.; Kariyeva, J. The synergistic use of RADARSAT-2 ascending and descending images to improve surface water detection accuracy in Alberta, Canada. *Can. J. Remote Sens.* **2019**, *45*, 759–769. [CrossRef]
33. Natural Regions Committee. *Natural Regions and Subregions of Alberta*; Downing, D.J., Pettapiece, W.W., Eds.; Government of Alberta: Edmonton, AB, Canada, 2006.
34. Environment Canada. Medicine Hat Historical Weather. Available online: https://climate.weather.gc.ca/historical_data/search_historic_data_e.html (accessed on 18 May 2021).
35. Winter, T.C.; Rosenberry, D.O. The interaction of ground water with prairie pothole wetlands in the Cottonwood Lake area, east-central North Dakota, 1979–1990. *Wetlands* **1995**, *15*, 193–211. [CrossRef]
36. Huang, S.; Dahal, D.; Young, C.; Changder, G.; Liu, S. Integration of Palmer Drought Severity Index and remote sensing data to simulate wetland water surface from 1910 to 2009 in Cottonwood Lake area, North Dakota. *Remote Sens. Environ.* **2011**, *115*, 337–3389. [CrossRef]
37. Alberta Biodiversity Monitoring Institute and Alberta Human Footprint Monitoring Program. *Alberta Biodiversity Monitoring Institute and Alberta Human Footprint Monitoring Program Wall-to-Wall Human Footprint Inventory 2018*; Alberta Biodiversity Monitoring Institute and Alberta Human Footprint Monitoring Program: Edmonton, AB, Canada, 2020; p. 145.
38. Esri. "Light Gray Canvas" [Baselayer]. Scale not Given. Created: 26 September 2011. Available online: https://www.arcgis.com/home/item.html?id=8b3d38c0819547faa83f7b7aca80bd76 (accessed on 23 May 2022).

39. Potapov, P.; Li, X.; Hernandez-Serna, A.; Tyukavina, A.; Hansen, M.C.; Kommareddy, A.; Pickens, A.; Turubanova, S.; Tang, H.; Silva, C.E. Mapping global forest canopy height through integration of GEDI and Landsat data. *Remote Sens. Environ.* **2021**, *253*, 112165. [CrossRef]
40. Achanta, R.; Susstrunk, S. Superpixels and Polygons Using Simple Non-Iterative Clustering. In Proceedings of the IEEE Conference on Computer Vision and Pattern Recognition, Honolulu, HI, USA, 21–25 July 2017.
41. Breiman, L.; Friedman, J.; Stone, C.J.; Olshen, R.A. *Classification and Regression Trees*; Routeledge: New York, NY, USA, 1984; p. 368. [CrossRef]
42. Esri. "Terrain with Labels" [Baselayer]. Scale not Given. Created: 9 June 2016. Available online: https://www.arcgis.com/home/item.html?id=a52ab98763904006aa382d90e906fdd5 (accessed on 23 May 2022).
43. Esri. "World Imagery" [Baselayer]. Scale not Given. Created: 12 December 2009. Available online: https://www.arcgis.com/home/item.html?id=10df2279f9684e4a9f6a7f08febac2a9 (accessed on 23 May 2022).
44. Hardy, A.; Oakes, G.; Ettritch, G. Tropical Wetland (TropWet) Mapping Tool: The Automatic Detection of Open and Vegetated Waterbodies in Google Earth Engine for Tropical Wetlands. *Remote Sens.* **2020**, *12*, 1182. [CrossRef]
45. Pekel, J.-F.; Cottam, A.; Gorelick, N.; Belward, A.S. High-resolution mapping of global surface water and its long-term changes. *Nature* **2016**, *540*, 418–422. [CrossRef]
46. ABMI Wetland Inventory. Available online: https://abmi.ca/home/data-analytics/da-top/da-product-overview/Advanced-Landcover-Prediction-and-Habitat-Assessment--ALPHA--Products/ABMI-Wetland-Inventory.html (accessed on 23 May 2022).